

Temperature Dependence of Excitonic Radiative Decay in CdSe Quantum Dots: The Role of Surface Hole Traps

Marco Califano, Alberto Franceschetti, and Alex Zunger*

National Renewable Energy Laboratory, Golden, Colorado 80401

Received June 2, 2005; Revised Manuscript Received September 30, 2005

ABSTRACT

Using atomistic, semiempirical pseudopotential calculations, we show that if one assumes the simplest form of a surface state in a CdSe nanocrystal—an unpassivated surface anion site—one can explain theoretically several puzzling aspects regarding the observed temperature dependence of the radiative decay of excitons. In particular, our calculations show that the presence of surface states leads to a mixing of the dark and bright exciton states, resulting in a decrease of 3 orders of magnitude of the dark-exciton radiative lifetime. This result explains the persistence of the zero-phonon emission line at low temperature, for which thermal population of higher-energy bright-exciton states is negligible. Thus, we suggest that surface states are the controlling factor of dark-exciton radiative recombination in currently synthesized colloidal CdSe nanocrystals.

Colloidally synthesized CdSe quantum dots have a high photoluminescence (PL) quantum yield reaching up to 85% even at room temperature,¹ indicating that nonradiative decay channels are weak and spurring interest in various optoelectronic applications such as diodes² and lasers.³ This motivated numerous recent experimental studies on the PL decay mechanisms in these systems,^{4–13} where a multiexponential PL decay was evidenced in ensembles of CdSe nanocrystals of different sizes.^{5,8,12,13} The temperature dependence of the long-time PL decay is usually interpreted in terms of a three-level system: the electronic ground state, a lower-energy “dark” (i.e., optically forbidden) exciton state X_D , and a higher-energy “bright” (i.e., optically allowed) exciton state X_B . The dark and bright excitons are separated by the exchange splitting Δ , which is of the order of a few meV in CdSe quantum dots in the nanometer size range. The high-temperature ($T > 10$ K) PL decay time can then be explained by thermal population of the bright exciton state, which is expected to have an intrinsic radiative lifetime of ~ 10 ns. The low-temperature ($T < 10$ K) PL decay, however, reveals a number of puzzling features (Figure 1, circles): (i) Measurements show a decay time τ of ~ 1 μ s at $T \sim 1$ K.⁸ This is surprising, because the dark exciton is expected¹⁴ to have a much longer radiative recombination lifetime. (ii) The saturation temperature T_0 (corresponding to the “kink” in the experimental $\tau(T)$ curve, shown in Figure 1) is nearly size-independent. Since T_0 depends on the exchange splitting

Δ , which increases with decreasing size, one would expect T_0 to increase as the size of the quantum dot is reduced.

Fluorescence line narrowing experiments¹⁵ have shown that, as the temperature decreases, the intensity of the one-phonon and two-phonon replicas in the emission spectrum increases at the expenses of the zero-phonon line. This observation has led to the suggestion that the dominant decay channel for dark excitons consists of phonon-assisted radiative recombination.^{14,15} This mechanism may explain the microsecond low-temperature radiative lifetime. However, the persistence of the zero-phonon line at temperatures below 2 K¹⁵—at which thermal population of the bright-exciton states becomes negligible—suggests the presence of a *direct* radiative recombination channel for the dark exciton that has so far remained unexplained. In this work, we address theoretically the direct (i.e., not phonon assisted) radiative recombination lifetimes of the dark and bright excitons in CdSe nanocrystals ranging from 2 to 4 nm in diameter. We find that the bright exciton has a radiative lifetime of 10–15 ns, depending on size, which yields a room-temperature lifetime of 25–35 ns, in excellent agreement with experiment. This result supports the interpretation of the high-temperature PL lifetime as originating from thermal population of the bright exciton states. Furthermore, we find that in the presence of surface states—either neutral or positively charged—the dark exciton has a radiative lifetime of ~ 1 μ s, 3 orders of magnitude shorter than the radiative lifetime of a dark exciton in a fully passivated CdSe nanocrystal. This effect is found to originate from the surface-induced mixing of dark and bright excitons. We conclude that a non-phonon-

* To whom correspondence should be addressed. E-mail: alex_zunger@nrel.gov.

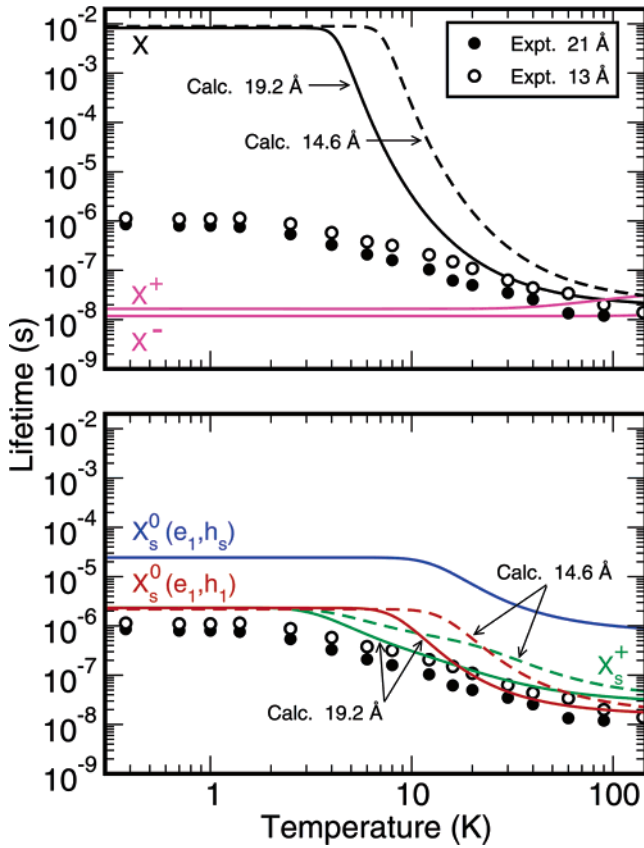


Figure 1. Calculated (lines) radiative lifetimes as a function of temperature for different exciton types (X , X^+ , X^- , X_s^+ , and X_s) in a $R = 19.2 \text{ \AA}$ (solid lines) and a $R = 14.6 \text{ \AA}$ (dashed lines) CdSe nanocrystal, compared with experimental data⁸ for $R = 13 \text{ \AA}$ (empty circles) and $R = 21 \text{ \AA}$ (solid circles). As in the experimental setup only the PL energy in a narrow bandwidth is collected, we considered only a limited number of thermally populated states with emission in a narrow (~ 8 – 12 meV) energy range, and since the experiment was carried out in the low-injection regime we did not include biexciton features.

assisted radiative recombination of the dark exciton, enabled by the presence of *surface* states, is responsible for the low-temperature lifetime of the zero-phonon PL peak.

The calculations were performed using a fully atomistic theory that accounts for many-body effects. We consider here nearly spherical wurtzite CdSe quantum dots of radius $R = 10.3, 14.6,$ and 19.2 \AA . The surface atoms were passivated by ligands.¹⁶ The hole and electron single-particle energies $\{\epsilon_{h,e}\}$ and wave functions $\{\psi_{h,e}\}$ were computed using the semiempirical nonlocal pseudopotential method (including spin–orbit effects) described in refs 17 and 18. The single-particle Schrodinger equation was solved in a plane-wave basis set. The many-body excitonic energies $\{E^{(i)}\}$ and wave functions $\{\Psi^{(i)}\}$ were expanded in terms of single-substitution Slater determinants $\{\Phi_{h,e}\}$, constructed from the single-particle wave functions of electrons and holes

$$\Psi^{(i)} = \sum_{h,e} C_{h,e}^{(i)} \Phi_{h,e} \quad (1)$$

The corresponding many-body Hamiltonian is solved within the framework of the configuration interaction (CI)

scheme. We use a position-dependent dielectric screening function for the direct and exchange Coulomb integrals. We expand the exciton states using $N_v = 30$ valence states and $N_c = 7$ conduction states, corresponding to CI basis sets of 840 configurations for neutral excitons and 24 780 configurations for positively charged excitons. More details on this procedure can be found in ref 18.

Previous quantitative pseudopotential calculations¹⁸ showed that X_B and X_D derive primarily from the lowest conduction state e_1 and the highest valence state h_1 (Figure 2a, upper panel), which, including spin, yield a 2×2 exciton manifold. This 4-fold exciton multiplet is split by exchange interactions into two 2-fold degenerate states (Figure 2a, lower panel): a lower energy, optically forbidden “dark” state X_D and a higher energy, optically allowed “bright” state X_B . Their radiative decay channel is indicated in the lower panel of Figure 2a (transitions labeled 1 and 2). X_D and X_B are separated by the electron–hole exchange splitting energy Δ , ranging from 5 to 16 meV for dots with sizes $R = 19.2$ – 10.3 \AA . Above the lowest X_D and X_B excitons are four exciton states derived from e_1 and h_2 . They have degeneracy of 1, 2, and 1 and are, respectively, dark, bright, and bright. As their separation from the lowest, e_1 – h_1 -derived excitons is of the order of 25–30 meV, the emission from these states (transitions labeled 3, 4, and 5 in Figure 2a) does not feature prominently in low-energy PL up to room temperature.

The radiative lifetime τ_i for the transition from the excitonic state $\Psi^{(i)}$ to the ground state is obtained in the framework of standard time-dependent perturbation theory as¹⁹

$$\frac{1}{\tau_i} = \frac{4nF^2\alpha\omega_i^3}{3c^2} |M_i|^2 \quad (2)$$

where α is the fine structure constant, n is the refractive index of the surrounding medium, $F = 3\epsilon/(\epsilon_{\text{dot}} + 2\epsilon)$ is the screening factor (here $\epsilon = n^2$ and ϵ_{dot} is the dielectric constant of the quantum dot), ω_i is the frequency of the emitted photon, c is the speed of light, and

$$M_i = \sum_{h,e} C_{h,e}^{(i)} \langle \psi_h | \mathbf{r} | \psi_e \rangle \quad (3)$$

is the dipole moment calculated between CI wave functions. Here we use the refractive index of toluene ($n = 1.496$). The dielectric constant of the dot is calculated using a modified Penn model;¹⁸ we find $\epsilon_{\text{dot}} = 4.8$ for $R = 10.3 \text{ \AA}$, 5.3 for $R = 14.6 \text{ \AA}$, and 5.6 for $R = 19.2 \text{ \AA}$. For $T > 0$, we calculate a thermally averaged lifetime by assuming Boltzmann occupation of higher-energy excitonic levels

$$\frac{1}{\langle \tau \rangle} = \frac{\sum_i (1/\tau_i) e^{-\Delta E_i/K_B T}}{\sum_i e^{-\Delta E_i/K_B T}} \quad (4)$$

Calculated room-temperature radiative lifetimes are in agreement with experiment: The lines marked “X” in Figure 1 show our calculated thermally averaged radiative lifetime

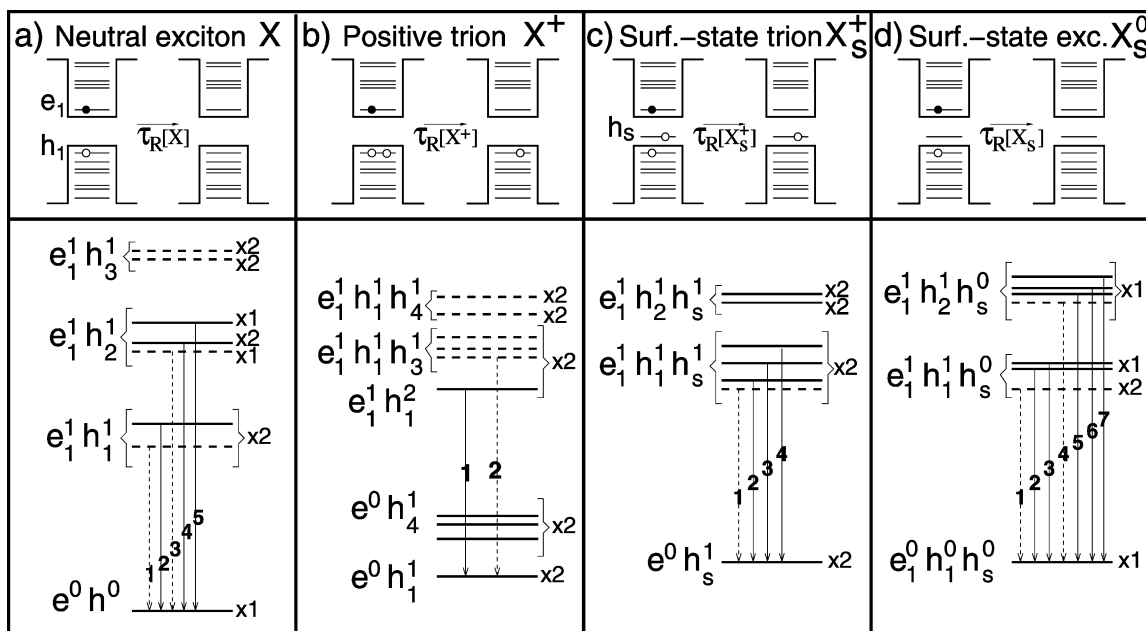


Figure 2. Schematics of our calculated single-particle (upper panels) and excitonic (lower panels) levels, for (a) neutral exciton X, (b) positive trion X^+ , (c) positive trion with a hole in a surface state X_s^+ , and (d) neutral exciton in the presence of a surface state X_s^0 . (lower panel) The notation $e^m h^j$ indicates that a specific exciton level is derived mainly from the single-particle levels e_i and h_j , occupied by m and j particles, respectively. Also, “ xn ” indicates that an exciton level has a degeneracy of “ n ”. Solid (dashed) horizontal lines indicate bright (dark) excitons, whereas vertical arrows indicate transitions between levels.

of the neutral exciton $\langle\tau(X)\rangle$ for two dot sizes as a function of temperature. We see that for $T > 10$ K, the lifetime $\langle\tau(X)\rangle$ is in good agreement with the experimental results.⁸ Figure 3 shows the high-temperature radiative lifetime $\langle\tau(X)\rangle$ as a function of size. Again, we find good agreement with experimental results^{4,7–9,11} over a range of sizes. By comparing our calculated thermal average $\langle\tau(X)\rangle$ with our calculated intrinsic bright radiative lifetimes $\tau(X_B)$, we find (Figure 3) that $\langle\tau(X)\rangle \approx 2\tau(X_B)$, in agreement with Labeau et al.⁹ This result shows that the high-temperature radiative lifetime is due to the thermal mixing of X_D and X_B , with higher excitonic states contributing less than 10%. We find that in the single-particle approximation (i.e., without CI) both $\langle\tau(X)\rangle$ and $\tau(X_B)$ increase with increasing nanocrystal size (i.e., decreasing energy gap). This trend is reversed—and the experimental behavior is recovered^{8,9}—only when correlations are taken into account in a full CI calculation. Interestingly, our results show a much slower decrease of $\tau(X_B)$ with increasing size than that predicted by the effective-mass approximation (EMA, black triangles in Figure 3). The difference is due to the inclusion in our calculations of intervalley coupling at the single-particle level (that is missing in simple EMA calculations), as well as configuration mixing at the excitonic level.

Low-temperature lifetimes are not explained by radiative recombination of charged excitons: At low temperatures ($T < 10$ K), we find that the calculated radiative lifetime of the neutral exciton is of the order of a few ms (Figure 1), which is significantly longer than the measured lifetime.^{8,9} The microsecond radiative lifetime of the dark exciton has been attributed^{9,15} to longitudinal optical phonon-assisted recombination. The persistence of the zero-phonon line at

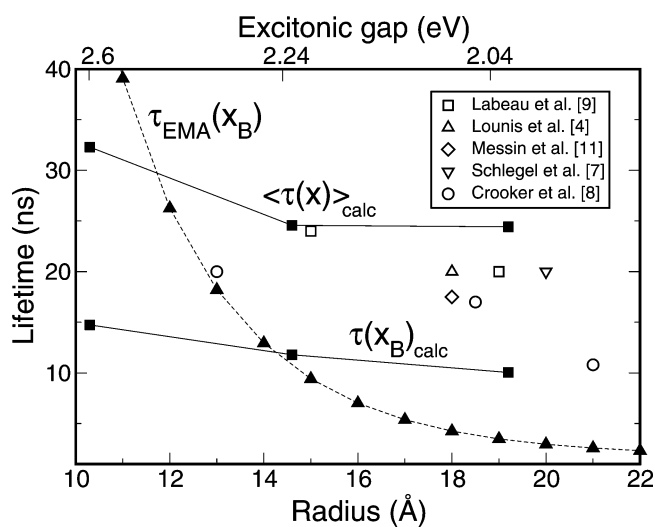


Figure 3. High-temperature experimental^{4,7–9,11} PL decay lifetimes (empty symbols), room-temperature radiative lifetimes $\langle\tau(X)\rangle$, and bright radiative lifetimes $\tau(X_B)$ calculated with the semiempirical pseudopotential method (black squares). Also shown is the bright-exciton radiative lifetime, $\tau_{\text{EMA}}(X_B)$, calculated in the effective-mass approximation. For the EMA calculation, we used eq 2 where the dipole matrix elements M_i were taken from ref 14. All experimental data refer to single nanocrystals in the single-exponential decay regime with the exception of those by Crooker et al.⁸ (circles), which are relative to ensemble measurement at long decay times. On the upper x axis our calculated excitonic gap for the three sizes considered here is shown.

low temperatures,¹⁵ however, suggests that there may be other mechanisms that contribute to the enhancement of the radiative recombination rate of the dark state. Javier and co-workers⁶ explained their observed biexponential PL decay in single nanocrystals in terms of a superposition of the decay

of neutral and charged excitons with similar lifetimes. Moreover, electrostatic force microscopy measurements performed on CdSe nanocrystals on insulator–metal substrates²⁰ found a positive charge on half of the investigated nanocrystals. These observations suggest that dark excitons in charged nanocrystals may have a different radiative recombination rate compared to neutral nanocrystals.

To test these ideas we calculated the excitonic manifold and the temperature-dependent radiative lifetimes of positively charged X^+ ($2h + 1e$) and negatively charged X^- ($1h + 2e$) excitons in CdSe nanocrystals. Figure 2b (lower panel) shows that the lowest energy state of X^+ is a 2-fold degenerate *bright* exciton²¹ derived from the $(e_1^1 h_1^2)$ single-particle configuration, followed by three 2-fold degenerate dark exciton states derived mainly from the $(e_1^1 h_1^1 h_1^3)$ configuration. Similarly, for X^- (not shown in Figure 2) the lowest energy exciton state is bright. The lowest energy transition in both X^+ and X^- is therefore optically allowed and has a short lifetime (~ 10 ns). As a result, our calculated $\langle\tau(X^+)\rangle$ and $\langle\tau(X^-)\rangle$ exhibit an almost T -independent value of ~ 10 ns, as shown in Figure 1. We conclude that charged excitons, where the charge resides in the dot interior, do not explain the behavior of the measured lifetimes at low temperature.

The presence of surface states reduces the radiative lifetime of dark excitons: The removal of a passivant from a surface Se atom creates a surface state that can be either in the gap or resonant with the valence band.²² The removal of a passivant from a surface Cd atom leads instead to surface states that are resonant with the conduction band or at its edge.²² In this work we investigate the effects of hole traps on exciton recombination, so we consider only surface states obtained by removing Se-passivating atoms. We have previously studied the consequences of unpassivated surface anions on the optical spectrum of CdSe²³ and InP²⁴ nanocrystals. In particular, we found that an unpassivated Se atom located on the $(000\bar{1})$ Se-terminated facet of a 19.2 Å radius CdSe nanocrystal leads to a surface-localized hole-trap state in the band gap,²³ a feature that was subsequently confirmed experimentally.²⁵ Given that such unpassivated Se atoms result in a large density of surface states in the band gap,²² we consider them as a likely source of surface hole traps. Parts c and d of Figure 2 depict the excitonic manifolds and the relevant radiative transitions in the presence of a neutral (X_s^0 , Figure 2d) or positively charged (X_s^+ , Figure 2c) surface state. The excitonic manifold calculated for X_s^0 (Figure 2d, lower panel) is very similar to that of X (Figure 2a): in both cases the lowest four excitonic states are derived from the $(e_1^1 h_1^1)$ configuration, and the following four from $(e_1^1 h_2^1)$. Also, the energy spacings between the ground state and the higher energy levels are almost identical in X and X_s^0 . The difference, however, lies in the degeneracy of these levels. Only the ground state exciton is doubly degenerate in X_s^0 , whereas the higher energy levels that were doubly degenerate in X are now split (by less than 2 meV) into singly degenerate states. Therefore we find that the transition energies of X , labeled 1–5 in Figure 2a, are very close to the corresponding ones in X_s^0 , labeled 1–7, in Figure 2d. The calculated

excitonic manifold of X_s^+ ²⁶ is composed of four 2-fold-degenerate levels that derive mainly from the single-particle $(e_1^1 h_s^1 h_1^1)$ configuration (Figure 2c, lower panel). Unlike the case of X^+ , we find that the lowest exciton state of X_s^+ is dark. Above the dark state we find three doubly degenerate bright states whose decay times to the ground state (transitions labeled 2, 3, and 4 in Figure 1c) are in the range 100–10 ns (i.e., decreasing with increasing energy separation from the dark exciton state) and are similar for the $R = 19.2$ Å and the $R = 14.6$ Å nanocrystals. The crucial features of the excitonic spectrum of X_s^+ , however, are that the separation between the dark state and the first bright state is (i) very small (1 meV) and (ii) identical in both dots. Furthermore (iii) the separation between the dark state and the third bright state of the bright multiplet is 8 meV (12 meV) in a $R = 19.2$ Å ($R = 14.6$ Å) nanocrystal. We consider thermal occupation of higher levels and calculate the temperature-dependent radiative lifetimes $\langle\tau(X_s^0)\rangle$ and $\langle\tau(X_s^+)\rangle$ (shown in Figure 1), from which we draw the following conclusions:

First, we find that the *presence* of a surface state, regardless of whether it is neutral or charged, lowers the symmetry of the system, leading to a mixing between forbidden and allowed excitonic states. This results in an enhancement of the dark exciton decay rate and a reduction of the bright decay rate, compared to the case of a perfectly passivated nanocrystal. The magnitude of the dark–bright exciton mixing depends on the orbital character and the degree of localization of the surface state, which in the case considered here originates mainly from the Se 4p orbitals and extends into the core of the nanocrystal. Our calculated lifetimes for the dark X_s^+ and X_s^0 excitons are both ~ 1 μ s and are similar for the dot sizes considered here ($R = 14.6$ Å and $R = 19.2$ Å). This is a 3 orders of magnitude decrease in the radiative lifetime, compared to an exciton in a fully passivated dot with no surface states. The presence of a surface gap state in a neutral dot (Figure 2d) can lead to hole capture, if the hole trapping time is shorter than the exciton radiative lifetime. Interestingly, we find that the recombination of a delocalized electron with a surface hole in a neutral dot also has a rather short (~ 10 μ s at $T = 0$) lifetime (curve labeled X_s^0 (e_1, h_s) in Figure 1).

Second, the saturation temperature T_0 for $\langle\tau(X_s^+)\rangle$ is approximately the same for the two dot sizes considered and is lower than that calculated for $\langle\tau(X)\rangle$ (Figure 1). This can be explained by the fact that the calculated energy splitting between dark and bright excitons in a charged dot with a surface state (Figure 2c) is ~ 1 meV for both $R = 19.2$ and $R = 14.6$ Å nanocrystals. Interestingly, the ~ 13 meV red shift observed in the PL for temperatures lower than 4 K in a $R = 13$ Å nanocrystal (and adduced⁸ as a proof of phonon coupling to explain fast decay of the dark exciton) is close to the energy splitting between the dark state and the bright state with higher oscillator strength, which we calculate to range from 8 to 12 meV for $R = 19.2$ Å and a $R = 14.6$ Å nanocrystals, respectively.

Third, at high temperature the calculated radiative lifetime is almost unaffected by the presence of a surface state, i.e.,

$\langle\tau(X_s^0)\rangle \approx \langle\tau(X_s^+)\rangle \approx \langle\tau(X)\rangle$, and is consistent with the measured PL decay time. In the case of X_s^+ , this occurs because the main contribution to the thermally averaged lifetime $\langle\tau(X_s^+)\rangle$ at high temperature comes from all four band edge exciton states (dark and bright), as their energies are within 8–12 meV. Furthermore, since the decay times of the three bright states are close to $\tau(X_B)$ and their separation from the dark state is close to Δ , it follows that $\langle\tau(X_s^+)\rangle \approx \langle\tau(X)\rangle$ at high T . Similarly, we find that for X_s^0 $\langle\tau(X_s^0)\rangle \approx \langle\tau(X)\rangle$.

The effect of surface charges on the bright exciton lifetime was considered by Wang.²⁷ Using semiempirical pseudopotential calculations, Wang demonstrated that the electric field set up by a classic point charge located near the surface of a CdSe nanocrystal can substantially alter the distribution of the electron and hole wave functions. For example, in the case of a positive charge, the electron is attracted by the surface charge, while the hole moves in the opposite direction. As a result of the reduced overlap between electron and hole wave functions, the bright exciton lifetime was found to increase by up to 2–3 orders of magnitude, depending on the location of the surface charge.²⁷ Similar results were obtained from k.p calculations of excitons in the presence of an ionized acceptor localized at the surface of a ZnO nanocrystal.²⁸ The calculations of ref 27 suggest that the increase in the lifetime of the bright exciton due to charge separation may explain the existence of “off” periods in the PL (blinking) and that an Auger mechanism may not be needed to explain such off periods. However, the present calculations—which describe the effects of a surface charge via a defect wave function rather than a classic point charge—find that this effect increases the lifetime of bright excitons only by a factor of ~ 3 , thus being insufficient to explain blinking.

In summary, from Figure 1 it is clear that although the lifetimes of the different exciton states X , X^- , X^+ , X_s^0 , and X_s^+ at high temperature are similar, the specific excitonic configurations they originate from can be determined by examining the overall behavior at low temperature. Figure 1 shows that the mixing of dark and bright excitons induced by surface states leads to a 3 orders of magnitude decrease in the radiative lifetime of the dark exciton. This explains the radiative lifetime of the zero-phonon line observed at low temperatures.

Acknowledgment. The authors thank V. Klimov, P. Guyot-Sionnest and D. Vanmaekelbergh for valuable discussions. This work was supported by the US DOE-SC-BES under Contract No. DEAC36-98-GO10337.

References

- (1) Qu, L.; Peng, X. *J. Am. Chem. Soc.* **2002**, *124*, 2049.
- (2) Colvin, V. L.; Schlamp, M. C.; Alivisatos, A. P. *Nature* **1994**, *370*, 354.
- (3) Klimov, V. I.; et al. *Science* **2000**, *290*, 314.
- (4) Lounis, B.; et al. *Chem. Phys. Lett.* **2000**, *329*, 399.
- (5) Chamarro, M.; et al. *Phys. Rev.* **1996**, *B 53*, 1336.
- (6) Javier, A.; Magana, D.; Jennings, T.; Strouse, G. F. *Appl. Phys. Lett.* **2003**, *83*, 1423.
- (7) Schlegel, G.; Bohnenberger, J.; Potapova, I.; Mews, A. *Phys. Rev. Lett.* **2002**, *88*, 137401.
- (8) Crooker, S. A.; Barrick, T.; Hollingsworth, J. A.; Klimov, V. I. *Appl. Phys. Lett.* **2003**, *82*, 2793.
- (9) Labeau, O.; Tamarat, P.; Lounis, B. *Phys. Rev. Lett.* **2003**, *90*, 257404.
- (10) Fisher, B. R.; Eisler, H.-J.; Scott, N. E.; Bawendi, M. G. *J. Phys. Chem. B* **2004**, *108*, 143.
- (11) Messin, G.; et al. *Opt. Lett.* **2001**, *26*, 1891.
- (12) Bawendi, M. G.; Carrol, P.; Wilson, L.; Brus, L. E. *J. Chem. Phys.* **1992**, *96*, 946.
- (13) O’Neil, M.; Marohn, J.; McLendon, G. *J. Phys. Chem.* **1990**, *94*, 4356.
- (14) Al. Efros, L.; et al. *Phys. Rev. B* **1996**, *54*, 4843.
- (15) Nirmal, M.; Murray, C. B.; Bawendi, M. G. *Phys. Rev. B* **1994**, *50*, 2293. Nirmal, M.; Norris, D. J.; Kuno, M.; Bawendi, M. G.; Efros, A. L.; Rosen, M. *Phys. Rev. Lett.* **1995**, *75*, 3728.
- (16) Wang, L.-W.; Zunger, A. *Phys. Rev. B* **1996**, *53*, 9579.
- (17) Wang, L.-W.; Zunger, A. *Phys. Rev. B* **1995**, *51*, 17 398.
- (18) Franceschetti, A.; Fu, H.; Wang, L.-W.; Zunger, A. *Phys. Rev. B* **1999**, *60*, 1819.
- (19) Dexter, D. L. *Solid State Physics*; Academic Press Inc.: New York, 1958; Vol. 6, pp 358–361.
- (20) Krauss, T. D.; Brus, L. E. *Phys. Rev. Lett.* **1999**, *83*, 4840.
- (21) For charged excitons with N particles we define as “bright” (“dark”) optically allowed (forbidden) states for transitions from and to the $(N - 2)$ particles lowest energy (i.e., ground) state.
- (22) Hill, N. A.; Whaley, K. B. *J. Chem Phys.* **1994**, *100*, 2831.
- (23) Franceschetti, A.; Zunger, A. *Phys. Rev. B* **2000**, *62*, R16287.
- (24) Fu, H.; Zunger, A. *Phys. Rev. B* **1997**, *56*, 1496.
- (25) Lifshitz, E.; Glotzman, A.; Litvin, I. D.; Porteanu, H. *J. Phys. Chem. B* **2000**, *104*, 10449. Micic, O.; et al. *J. Phys. Chem. B* **2002**, *106*, 4390.
- (26) We consider the process $e_1h_3h_1 \rightarrow h_s$, i.e., the recombination of the electron and hole in the dot core. We find that the radiative decay rate for the alternative process $e_1h_3h_1 \rightarrow h_1$ (recombination of a core electron with a surface hole) is 1 to 3 orders of magnitude smaller than that for $e_1h_3h_1 \rightarrow h_s$.
- (27) Wang, L. W. *J. Phys. Chem. B* **2001**, *105*, 2360.
- (28) Fonoberov, V. A.; Balandin, A. A. *Appl. Phys. Lett.* **2004**, *85*, 5971.

NL051027P